



Promising application of polyoxometalates in the treatment of cancer, infectious diseases and Alzheimer's disease

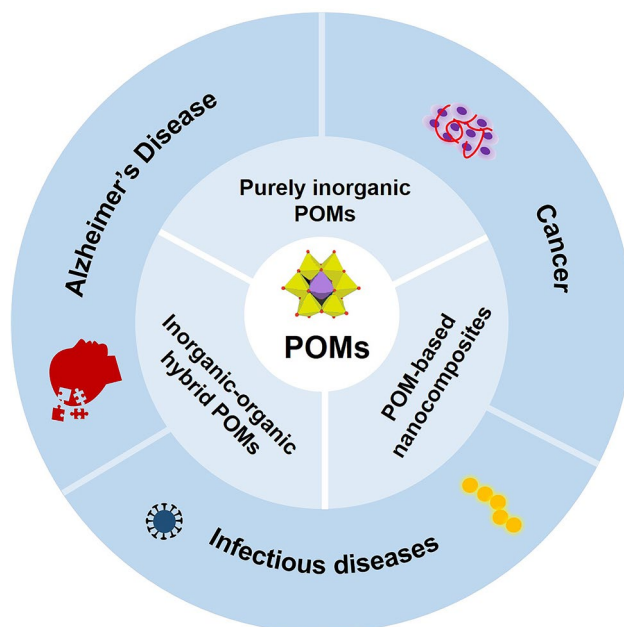
Xuechen Wang¹ · Shengnan Wei¹ · Chao Zhao¹ · Xin Li¹ · Jin Jin¹ · Xuening Shi¹ · Zhenyue Su¹ · Juan Li¹ · Juan Wang¹

Received: 24 November 2021 / Accepted: 9 May 2022 / Published online: 17 June 2022
© The Author(s), under exclusive licence to Society for Biological Inorganic Chemistry (SBIC) 2022

Abstract

As shown in studies conducted in recent decades, polyoxometalates (POMs), as inorganic metal oxides, have promising biological activities, including antitumor, anti-infectious and anti-Alzheimer's activities, due to their special structures and properties. However, some side effects impede their clinical applications to a certain extent. Compared with unmodified POMs, POM-based inorganic–organic hybrids and POM-based nanocomposite structures show significantly enhanced bio-activity and reduced side effects. In this review, we introduce the biological activities of POMs and their derivatives and highlight the side effects of POMs on normal cells and organisms and their possible mechanisms of action. We then propose a development direction for overcoming their side effects. POMs are expected to constitute a new generation of inorganic metal drugs for the treatment of cancer, infectious diseases, and Alzheimer's disease.

Graphical abstract



Keywords Biological activity; POMs · Cancer · Infectious diseases · Alzheimer's disease

Xuechen Wang and Shengnan Wei have contributed equally.

Extended author information available on the last page of the article

Abbreviations

A549	Human non-small-cell lung cancer cell line	HFFs	Primary human foreskin fibroblasts
AChE	Acetylcholinesterase	HIV	Human immunodeficiency virus
AD	Alzheimer's disease	HL-60	Leukemia cell line
AgNPsY	Tyrosine-reduced AgNPs	HLC	Colon cancer cell line
AgPW	$\text{Ag}_3\text{PW}_{12}\text{O}_{40}$	HMC	Normal human kidney inherent cell line
AIDS	Acquired immunodeficiency syndrome	HMONs	Hollow mesoporous organosilica nanoparticles
AsPC-1	Human pancreatic cancer cell line	HPA-23	$(\text{NH}_4)_{17}\text{Na}(\text{NaSb}_9\text{W}_{21}\text{O}_{86})$
AuNPsTyr	Tyrosine-reduced AuNPs	HPBCs	Human peripheral blood cell line
$A\beta$	Amyloid β peptide	HSV	Herpes simplex virus
B	Boron	Huh7.5.1	Human lung cancer cell line
B16	Mouse melanoma cell line	HUVECs	Human umbilical vein endothelial cell line
B16F17	Murine melanoma cell line	IC ₅₀	50% Inhibitory concentration
BBB	Blood–brain barrier	JEV	Japanese encephalitis virus
BEAS-2B	Human normal bronchial epithelial cell line	KB	Human oral epidermoid cancer cell line
C2C12	Normal murine/mouse myoblast cell line	KCN	One of neuroblastoma cell line
CA	Cholic acid	L929	Normal murine fibroblast cell line
CADO-ES-1	Ewing's sarcoma cell line	LD ₅₀	Median lethal dose
CMC	Carboxymethyl chitosan	LEP	Liposome-encapsulated polyoxometalate
Cp	$\eta^5\text{-C}_5\text{H}_5$	MA-104	Embryonic African green monkey kidney cell line
CTS-P5W30	Chitosan- $[\text{NaP}_5\text{W}_{30}\text{O}_{110}]^{14-}$	MBC	Minimum bactericidal concentration
DENV	Dengue virus	MC3T3-E1	Normal osteoblast cell line
DHCA	Dehydrocholic acid	MCF-10A	Noncancerous breast epithelial cell line
DSPE-PEG2000	1,2-Distearoyl-sn-glycero-3-phosphoethanolamine- <i>N</i> -[methoxy (polyethylene glycol)-2000]	MCF-7	Breast cancer cell line
EC50	Median effective concentration	MDA-MB-231	Breast cancer cell line
EuWA	$[\text{Cs} \subset \text{Eu}_6\text{As}_6\text{W}_{63}\text{O}_{218}(\text{H}_2\text{O})_{14}(\text{OH})_4]^{25-}$	MDCK	Markedly cytotoxic in canine kidney cell line
FLaPW	$\text{K}_9(\text{C}_4\text{H}_4\text{FN}_2\text{O}_2)_2\text{La}(\text{PW}_{11}\text{O}_{39})_2 \cdot 18\text{H}_2\text{O}$	MG-63	Human osteosarcoma cell line
FluV A/B	Influenza virus A/B	MIC	Minimum inhibitory concentration
FMN	Flavin mononucleotide	Mo	Molybdenum
FNdPW	$\text{K}_9(\text{C}_4\text{H}_4\text{FN}_2\text{O}_2)_2\text{Nd}(\text{PW}_{11}\text{O}_{39})_2 \cdot 25\text{H}_2\text{O}$	MRSA	Staphylococcus aureus
FNSW	$\text{K}_{26}(\text{C}_4\text{H}_4\text{FN}_2\text{O}_2)_8\text{Nd}(\text{SiW}_{11}\text{O}_{39})_4 \cdot 5\text{H}_2\text{O}$	MSNs	Mesoporous silica nanoparticles
FSW	$\text{C}_4\text{H}_4\text{FN}_2\text{O}_2\text{H}_3\text{SiW}_{12}\text{O}_{40} \cdot 12\text{H}_2\text{O}$	NB	Niobium
FYPW	$\text{K}_{10}\text{C}_4\text{H}_4\text{FN}_2\text{O}_2\text{Y}(\text{PW}_{11}\text{O}_{39})_2 \cdot 10\text{H}_2\text{O}$	NIR	Near-infrared
GSH	Glutathione	P	Phosphorus
H. pylori	Helicobacter pylori	PBMC	Human peripheral blood mononuclear cells
HBV	Hepatitis B virus	PC-3	Human prostate cancer cell line
HCV	Hepatitis C virus	Pd13	$(\text{Na}_8[\text{Pd}_{13}\text{As}_8\text{O}_{34}(\text{OH})_6] \cdot 42\text{H}_2\text{O})$
HDAC	Histone deacetylase	PM-17	$[\text{Me}_3\text{NH}]_6[\text{H}_2\text{Mo}^{\text{V}}_{12}\text{O}_{28}(\text{OH})_{12}(\text{Mo}^{\text{VI}}\text{O}_3)_4] \cdot 3\text{H}_2\text{O}$
HDF- α	Human dermal fibroblasts	PM-19	$\text{K}_7(\text{PTi}_2\text{W}_{10}\text{O}_{40}) \cdot 6\text{H}_2\text{O}$
HEK293	Normal human embryonic kidney cell line	PM523	$(\text{IPrNH}_3)_6[\text{PTi}_2\text{W}_{10}\text{O}_{38}(\text{O}_2)_2] \cdot \text{H}_2\text{O}$
HeLa	Human cervical carcinoma cell line	PM-8	$[\text{NH}_3\text{Pri}]_6[\text{Mo}_7\text{O}_{24}] \cdot 3\text{H}_2\text{O}$
HEp-2	Human larynx epidermoid carcinoma cell line	PMA	12-Phosphomolybdic acid
HepG2	Human liver tumor cell line	POM	Polyoxometalates
		POM-1	$[(\text{CH}_3)_4\text{N}]_2\text{Na}_{6.5}(\text{NH}_4)_2[\text{Sn}^{\text{II}}_{1.5}(\text{WO}_2(\text{O} \text{H}))_{0.5}(\text{WO}_2)_2(\text{SbW}_9\text{O}_{33})_2] \cdot 32\text{H}_2\text{O}$
		POM-12	$\text{Cs}_2\text{K}_4\text{Na}[\text{SiW}_9\text{Nb}_3\text{O}_{40}] \cdot \text{H}_2\text{O}$

POM-2	$\text{Na}_{11}(\text{NH}_4)$ $[(\text{Mn}^{\text{II}}(\text{H}_2\text{O}))_3(\text{SbW}_9\text{O}_{33})_2]\cdot 45\text{H}_2\text{O}$
POM-3	$\text{Na}_5\text{K}_7[(\text{V}^{\text{IV}}\text{O})_3(\text{AsW}_9\text{O}_{33})_2]\cdot 29\text{H}_2\text{O}$
POM-4	$[(\text{CH}_3)_4\text{N}]_2\text{Na}_7[(\text{Mn}^{\text{III}}(\text{H}_2\text{O}))_3(\text{SbW}_9\text{O}_{33})_2]\cdot 24.5\text{H}_2\text{O}$
POM-5	$\text{Na}_{10}[\text{Mn}^{\text{II}}_2(\text{H}_2\text{O})_6(\text{WO}_2)_2(\text{SbW}_9\text{O}_{33})_2]\cdot 40\text{H}_2\text{O}$
POM-6	$\text{Na}_6[\text{Cu}_2^{\text{II}}(\text{H}_2\text{O}_2)_2(\text{H}_2\text{W}_{12}\text{O}_{42})]_{26}\cdot \text{H}_2\text{O}$
POM93	$\text{Cs}_2\text{K}_4\text{Na} [\text{SiW}_9\text{Nb}_3\text{O}_{40}]\cdot \text{H}_2\text{O}$
PTA	12-Phosphoric acid
PW_9Cu	$\text{K}_2\text{Na}_3[\text{Cu}_4(\text{H}_2\text{O})_2(\text{PW}_9\text{O}_{34})_2]_{20}\cdot \text{H}_2\text{O}$
ROS	Reactive oxygen species
rPOMs	Reduced POMs
RSV	Respiratory syncytial virus
Sb	Antimony
SHEP-SF	Neuroblastoma cell line
SH-SY5Y	Human neuroblastoma cells
Si	Silicon
$\text{Si}_2\text{W}_{18}\text{Ti}_6$	$\alpha\text{-K}_8\text{H}_6[\text{Si}_2\text{W}_{18}\text{Ti}_6\text{O}_{77}]$
SiW_{11}Ti	$\text{K}_6[\text{SiW}_{11}\text{TiO}_{40}]\cdot 16\text{H}_2\text{O}$
SK-ES-1	Human Ewing sarcoma cell line
SMMC-7721	Human liver cancer cell line
TBA-POM-biot ₂	$(\text{NBu}_4\text{N})_3\text{H}[\gamma\text{-SiW}_{10}\text{O}_{36}\{(\text{C}_5\text{H}_7\text{N}_2\text{O}_5)(\text{CH}_2)_4\text{CONH}(\text{CH}_2)_3\text{Si}\}_2\text{O}]$
TC ₅₀	Median toxic concentration
TMC	Trimethyl chitosan
Tris	Tris(hydroxymethyl)aminomethane
UMR106	Rat osteosarcoma cell line
V	Vanadium
VMOP-31	$(\text{NH}_2\text{Me}_2)_{12}[(\text{V}_5\text{O}_9\text{Cl})_6(\text{tatb})_8]$
VPLs	Virus-like particles
VRSA	Vancomycin-resistant <i>S. aureus</i>
W	Tungsten
WPA	12-Tungstophosphoric acid
WSiA	12-Tungstosilicic acid

X	Heteroatoms
ZIKV	Zika virus

Introduction

POMs are polyanionic oxides described as clusters of addenda atoms in their highest oxidation number, such as tungsten (W), molybdenum (Mo), niobium (Nb), antimony (Sb), and vanadium (V), with the eventual presence of heteroatoms [(X)], such as phosphorus (P), boron (B), and (or) silicon (Si), and linked by oxygen anions [1–5]. The three-dimensional structure of POMs is mainly composed of either corner-sharing (one bridging μ_2 -oxo group) or edge-sharing (two bridging μ_2 -oxo groups) of MO_6 octahedra [6]. POMs exhibit an overwhelming variety of shapes and sizes, including the Keggin- ($[\text{XM}_{12}\text{O}_{40}]^{n-}$), Wells–Dawson- ($[\text{X}_2\text{M}_{18}\text{O}_{62}]^{n-}$) and Anderson-type ($[\text{XM}_6\text{O}_{24}]^{n-}$) structures (Fig. 1) [7]. POMs are relatively stable with strong electron acceptance and transfer abilities, which allow the formation of derivatives with different structures via coupling with metal or organic groups [8]. The main advantage provided by POMs, which are programmable, is that the structure of metal oxide cluster anions can be designed and modified such that many elements can be easily introduced into the POM framework. Due to their unique properties, POMs show an overwhelming diversity in size, structure, and physicochemical capabilities, such as shape, redox potential, surface charge distribution, polarity, and acidity [4]. Their biologically relevant activity is closely related to their composition, shape, and size. In the 1980s, Jasmin et al. first found that ammonium 21-tungsto-9-antimoniate [HPA-23, $(\text{NH}_4)_{17}\text{Na}(\text{NaSb}_9\text{W}_{21}\text{O}_{86})$] could protect against DNA and RNA viruses [8, 9]. Many polyoxometalate derivatives have been synthesized and exhibit biological activities for tumor [5], viral [particularly human immunodeficiency virus (HIV) and hepatitis B virus (HBV)] [10], bacterial [11],

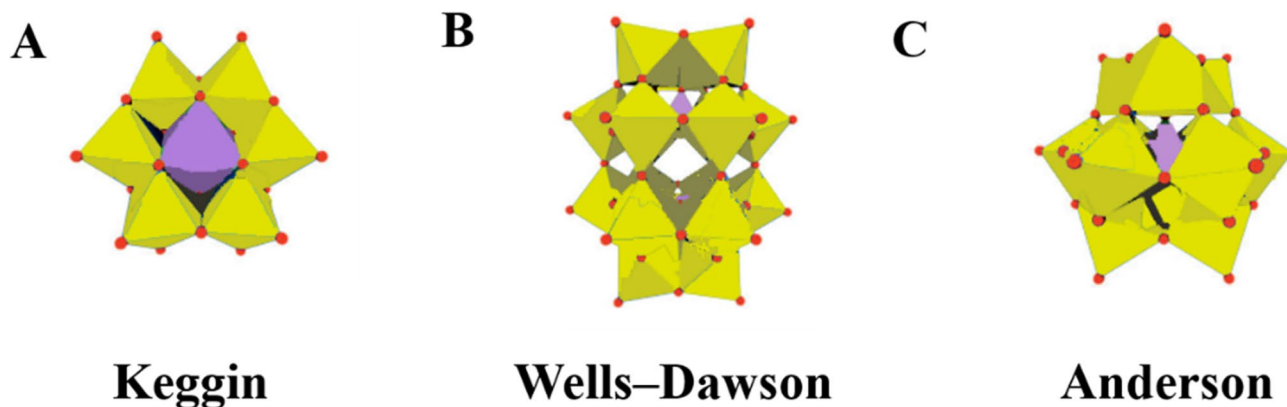


Fig. 1 Overview of POMs with the most common archetypes. A Keggin, B Wells–Dawson, C Anderson

and Alzheimer's disease (AD) therapy [12]. For example, $[\text{NH}_3\text{Pri}]_6[\text{Mo}_7\text{O}_{24}]\cdot 3\text{H}_2\text{O}$ (PM-8) significantly inhibits the growth of a variety of tumors, including the MX-1 murine mammary cancer, Meth A sarcoma and MM46 adenocarcinoma cell lines [13, 14]. The Keggin-type structure of polyoxotungstates demonstrates marked antiherpetic activity. Due to their benefits, the development of novel POMs for use as new drug candidates can be expected.

However, despite the successful application of certain POMs, most pure inorganic POMs exhibit high and long-term toxicity, which hinders their clinical applications. The development of POMs is limited by three main factors: (1) due to the special charge and structure of POMs, they exhibit severe toxic side effects at high dosages [1, 2]. (2) As negatively charged clusters, their surfaces are evenly distributed with tightly packed oxygen atoms, which leads to a generally weak and unspecific interaction between the POM and biomolecules [1]. (3) Most POM archetypes are thermodynamically and kinetically unstable, their conformational change depends on surrounding environmental factors, such as the solution concentration and the coexistence of foreign inorganic or organic matter, and at micromolar concentrations, POMs can be degraded into a mixture of smaller fragments at physiological pH [2–5].

Intriguingly, due to the tunability and physicochemical properties of the POM structure [15], different types of organic or inorganic groups can be easily introduced into the POM framework to modify and synthesize multiple functional compounds [4, 16–19]. Strategies such as encapsulation technology [15, 17] and the grafting of bioactive organic ligands onto the nuclei of inorganic POMs [20] have been used to minimize their toxicity and improve their bioactivity. Moreover, their lower cost and easier synthesis have made the medicinal properties of POMs the focus of attention [1, 10].

In this review, we provide a comprehensive overview of the biological activities of POMs and their potential biomedical applications in the treatment of cancer, infectious diseases, and AD and detail their possible toxic side effects on healthy cells (animals). In addition, we expound why POMs remain the potential next generation of clinical drugs despite their shortcomings.

Application of POMs in antitumor therapy

Application of purely inorganic POMs

POMs, a discrete cluster of metal oxide anions, have been studied to determine their potential pharmaceutical applications. POMs exhibit considerable potential as metallodrugs in antitumor therapy. However, their toxicity remains an unresolved issue, which impedes their clinical application.

In 1988, Yamase et al. found that the synthesis of PM-8 could inhibit the growth of tumors in different mouse models. PM-8 is somewhat more active than certain approved drugs, such as 5-fluorouracil (5-FU), in vitro and in vivo [21]. The toxicity of PM-8 is low despite application of a high dose of 250 mg/kg, and the mice maintained their weight for an average for 14 days [21]. In 1993, Yamase et al. proposed that the antitumor mechanism of PM-8 involves its reduction to $[\text{Me}_3\text{NH}]_6[\text{H}_2\text{Mo}^{\text{V}}_{12}\text{O}_{28}(\text{OH})_{12}(\text{Mo}^{\text{VI}}\text{O}_3)_4]\cdot 3\text{H}_2\text{O}$ (PM-17) and that PM-17 reduces and kills cancer cells [21]. Flavin mononucleotide (FMN) is a coenzyme for some oxidative enzymes and the principal form of riboflavin in cells and tissues and acts as an electron carrier for electron transfer (from NADH to coenzyme Q). During this process, the multielectron reduction of $[\text{Mo}_7\text{O}_{24}]^{6-}$ to PM-17 is biologically initiated through the one-electron reduction of the 1:1 $[\text{Mo}_7\text{O}_{24}]^{6-}$ -FMN complex that forms on the tumor cell mitochondria and results in suppression of tumor growth due to the inhibition of ATP generation [22]. The toxicity of PM-17 is significantly higher than that of PM-8. Treatment with 25 mg/kg PM-17 significantly inhibited the growth of Meth A sarcoma tumors on the 14th day. However, continuous administration of PM-17 could lead to body weight loss. It is possible that PM-17 is a reduced species of PM-8, and the toxic effects on weight appear to be associated with the production of PM-17 resulting from the 12-electron reduction of $[\text{Mo}_7\text{O}_{24}]^{6-}$ [21]. It has been suggested that PM-8 preferentially enters tumor cells and exerts its antitumor effects by forming PM-17 and inhibiting the formation of ATP. Furthermore, the toxicity of PM-17 in mice has been examined through hematological and serological analyses. No hepatic or renal dysfunction is observed with the administration of the therapeutic dose to human pancreatic cancer cells (AsPC-1) [22]. Despite the notable effects of PM-8 and PM-17, purely inorganic POMs may have long-term toxicity, which limits their clinical application in cancer therapy.

POM-1 to POM-6 ($[(\text{CH}_3)_4\text{N}]_2\text{Na}_{6,5}(\text{NH}_4)_2[\text{Sn}^{\text{I}}_{1.5}(\text{WO}_2(\text{OH}))_{0.5}(\text{WO}_2)_2(\text{SbW}_9\text{O}_{33})_2]\cdot 32\text{H}_2\text{O}$, POM-1; $\text{Na}_{11}(\text{NH}_4)[(\text{Mn}^{\text{II}}(\text{H}_2\text{O}))_3(\text{SbW}_9\text{O}_{33})_2]\cdot 45\text{H}_2\text{O}$, POM-2; $\text{Na}_5\text{K}_7[(\text{V}^{\text{IV}}\text{O})_3(\text{AsW}_9\text{O}_{33})_2]\cdot 29\text{H}_2\text{O}$, POM-3; $[(\text{CH}_3)_4\text{N}]_2\text{Na}_7[(\text{Mn}^{\text{III}}(\text{H}_2\text{O}))_3(\text{SbW}_9\text{O}_{33})_2]\cdot 24.5\text{H}_2\text{O}$, POM-4; $\text{Na}_{10}[\text{Mn}^{\text{II}}_2(\text{H}_2\text{O})_6(\text{WO}_2)_2(\text{SbW}_9\text{O}_{33})_2]\cdot 40\text{H}_2\text{O}$, POM-5; $\text{Na}_6[\text{Cu}_2^{\text{II}}(\text{H}_2\text{O})_2(\text{H}_2\text{W}_{12}\text{O}_{42})]_{26}\cdot \text{H}_2\text{O}$, POM-6), particularly POM-1 and POM-2, exert stronger biological effects against malignant cell lines, particularly platinum-resistant cell lines, and thus have a more promising future in cancer treatment compared with standard anticancer drugs such as cisplatin and carboplatin [23]. POM-1 is more cytotoxic than cisplatin in a neuroblastoma cell line (KCN) and an Ewing's sarcoma cell line (CADO-ES-1) but not in hepatocellular carcinoma or renal cancer cell lines. POM-2 has a very similar median lethal dose (LD_{50}) for neuroblastoma cell lines (SHEP-SF, KCN) and CADO-ES-1 in the

range of 6.85 to 9.84 μM [24]. POM-1 can suppress tumor growth by inhibiting the activity of NTPDase, and no significant liver or renal toxicity is observed at the suppressive dose (Table S1) [25]. However, all six abovementioned POMs are stable in the body and not easily metabolized, which results in toxic effects. In 2021, Liu et al. reported hierarchically structured giant polyoxometalate superclusters, $(\text{NH}_2\text{Me}_2)_{22}\text{K}_{12}\text{Na}_{12}[(\text{Sn}(\text{CH}_3)_2)_2\text{O}]_4\{[\text{CeW}_5\text{O}_{18}][\text{TeW}_4\text{O}_{16}]_4[\text{Ce}(\text{Sn}(\text{CH}_3)_2)_4[\text{TeW}_8\text{O}_{31}]_4\}_2 \cdot \text{ca.}186\text{H}_2\text{O}$. This compound shows obvious cytotoxicity against human cervical carcinoma cell line (HeLa), breast cancer cell line (MCF-7), human liver tumor cell line (HepG2), human non-small-cell lung cancer cell line (A549), human liver cancer cell line (SMMC-7721), and murine melanoma cell line (B16F17). Notably, this compound is also highly toxic to kidney epithelial cells according to the MTT assay [26]. Consequently, the application of this compound in cancer treatment is limited by its toxicity. The most effective way to solve this problem is to improve its cancer-specific targeting.

With good antitumor properties, purely inorganic POMs also exhibit inherent toxicity to the body or normal cells. Due to the charge, polarity and redox properties of most POM surfaces, POMs show poor biocompatibility and relatively low stability under physiological conditions. Additionally, the surface features of POMs limit their infiltration into cells [27]. As a result, POMs are not easily excreted or expurgated from the body, leading to long-term toxicity [28]. POMs may also bind to proteins through high-affinity electrostatic interactions, which possibly blocks the cell cycle and binding to proteins in cells and may thereby result in potential cytotoxicity [27, 29]. For example, various POMs identify and inhibit different kinases, including hexokinase, phosphofructokinases, and protein kinase CK2, in a noncompetitive manner [30]. Protein kinases are generally upregulated in many cancer cells, and their inhibition has been suggested a potential mechanism contributing to the antiapoptotic and anticancer effects of POMs. In addition, some POMs could be identified as histone deacetylase (HDAC) inhibitors that inhibit the growth of cancer cells [31]. To reduce the cytotoxicity of POMs on normal cells, it is worth exploring the structure–activity relationships of POMs and methods for enhancing their biological targeting. Consequently, the modification of purely inorganic POMs, such as through organic–inorganic hybrid-based functionalization or encapsulation and POM-based nanocomposites, could significantly reduce the toxicity of POMs and improve their antitumor activity. Moreover, it has been reported that POMs and copper (II) can form the compound $\text{K}_7\text{Na}_3[\text{Cu}_4(\text{H}_2\text{O})_2(\text{PW}_9\text{O}_{34})_2]_{20} \cdot \text{H}_2\text{O}$ (PW_9Cu). This compound is cytotoxic to a human osteosarcoma cell line (MG-63) and a rat osteosarcoma cell line (UMR106). The abovementioned experiment revealed a more serious

antiproliferative effect of PW_9Cu in MG-63 cells than in a normal osteoblast cell line (MC3T3-E1). The main mechanism of the toxicity of PW_9Cu to cells is the production of reactive oxygen species (ROS) and a reduction in glutathione (GSH) levels [18].

Application of inorganic–organic hybrid POMs

When modified by organic groups, POMs can exhibit reduced toxic side effects. Changes in the surface structure, charge and polarity of POM-based inorganic–organic hybrids lead to improved cell penetration, increased selectivity, and decreased toxicity.

The first reported organometallic polyoxometalate, $[\text{PW}_{11}\text{O}_{39}(\text{TiCp})]^{4-}$ (Cp: $\eta^5\text{-C}_5\text{H}_5$), forms a complete class of organometallic compound derivatives [19]. In 2003, J Liu et al. investigated POMs containing organometallic groups, that is, polyoxotungstate $[\text{CoW}_{11}\text{O}_{39}(\text{CpTi})]^{7-}$. The anion $\text{CoW}_{11}(\text{CpTi})$ can inhibit the growth of many types of tumor cells, including colon cancer cell line (HLC), leukemia cell line (HL-60) and SMMC-7721 cell line. The antitumor activity of $\text{CoW}_{11}(\text{CpTi})$ is similar to that of cyclophosphamide and 5-FU, but the cytotoxicity of $\text{CoW}_{11}(\text{CpTi})$ is significantly lower than that of 5-FU. The IC_{50} (50% inhibitory concentration) of $\text{CoW}_{11}(\text{CpTi})$ against SMMC-7721 and HeLa cells lines are only 3.2 and 11.5 μM , respectively. However, the IC_{50} values for peripheral lymphocyte cells and marrow cells are 442 and 730 mM, respectively. In vitro and in vivo experiments have shown that $\text{CoW}_{11}(\text{CpTi})$ is less toxic. In mice, the LD_{50} of $\text{CoW}_{11}(\text{CpTi})$ is 2898 mg/kg with a 95% confidence limit (95% CI) of 2792–3004 mg/kg [19]. In 2020, Joshi A et al. reported a Strandberg-type POM ($[\text{HP}_2\text{Mo}_5\text{O}_{23}]^{5-}$) functionalized with a flexible organic ligand, 4,4'-bipyridine (4,4'- H_2bpy), to form $\{[4,4'\text{-H}_2\text{bpy}]\}_2\{[\text{H}_2\text{P}_2\text{Mo}_5\text{O}_{23}]\} \cdot 5\text{H}_2\text{O}$. This hybrid POM has higher stability and exerts a synergistic effect in tumor treatment [26]. The cytotoxic effect of this compound has been studied in vitro on normal murine fibroblast cell line (L929). The ligand alone ($\text{IC}_{50} = \sim 40\text{ }\mu\text{M}$) is more toxic to normal cells than the synthesized compound ($\text{IC}_{50} > 100\text{ }\mu\text{M}$). The results showed that $[\text{HP}_2\text{Mo}_5\text{O}_{23}]^{5-}$ reduces the toxicity of this organic ligand. The IC_{50} values obtained for HepG2, A549 and MCF-7 cell lines are 33.79 μM , 25.17 μM , and 32.11 μM , respectively. In addition, the researchers investigated the mechanism of its antitumor effect and concluded that the compound might regulate apoptosis and necrosis pathways [32]. Interestingly, Xue et al. constructed a novel bioinorganic hybrid system, $[\text{Mo154}]@\text{VLPs}$, using virus-like particles (VLPs) of the human papilloma virus capsid protein L1 and molybdenum-containing polyoxometalate of $[\text{Mo154}]$. An MTT assay was employed to investigate the survival rate of $[\text{Mo154}]@\text{VLPs}$ on normal human embryonic kidney cell line (HEK293). The results showed that

90% and 82% cell viability are maintained with 50 μM and 10 μM [Mo154]@VLPs, respectively. Therefore, [Mo154]@VLPs are slightly cytotoxic to HEK293 cells [33].

POMs combined with drug molecules are also popular for tumor treatment because drugs are more selective and less toxic. 5-FU is a widely used anticancer drug but exhibits obvious defects, such as toxicity to marrow, severe gastrointestinal reactions and low selectivity [34]. Combining 5-FU with POMs significantly improves the selectivity. For example, the combination of 5-FU with the Keggin POM $[\text{PW}_{12}\text{O}_{40}]^{3-}$ exhibits lower toxicity than the free drug on HEK293 cells [35]. W was selected over Mo due to its remarkable redox stability [36]. The LD_{50} of the new compound $(\text{C}_4\text{H}_3\text{FN}_2\text{O}_2)_3\text{HSi}\cdot\text{W}_{12}\text{O}_{40}\cdot 3\text{H}_2\text{O}$ is 1158.25 mg/kg (95% CI 1072.87–1596.54 mg/kg). The toxicity of this compound is significantly lower than that of 5-FU and pure POM [37]. Two rare earth-substituted Keggin-type polyoxometalate compounds, $\text{K}_{10}\text{C}_4\text{H}_4\text{FN}_2\text{O}_2\text{Y}(\text{PW}_{11}\text{O}_{39})_2\cdot 10\text{H}_2\text{O}$ (FYPW) and $\text{K}_9(\text{C}_4\text{H}_4\text{FN}_2\text{O}_2)_2\text{La}(\text{PW}_{11}\text{O}_{39})_2\cdot 18\text{H}_2\text{O}$ (FLaPW), have similar toxicities but higher antitumor activities than 5-FU against HeLa and HepG2 cells at the same dose [35]. The rare earth elements Nd and 5-FU have been combined with tungstosilicic polyoxometalate to form $\text{K}_{26}(\text{C}_4\text{H}_4\text{FN}_2\text{O}_2)_8\text{Nd}(\text{SiW}_{11}\text{O}_{39})_4\cdot 5\text{H}_2\text{O}$ (FNSW). FNSW has lower cytotoxicity in HEK293 cell line (median toxic concentration (TC_{50}) = 45.9 μM) than 5-FU (TC_{50} = 14.7 μM) and $\text{C}_4\text{H}_4\text{FN}_2\text{O}_2\text{H}_3\text{SiW}_{12}\text{O}_{40}\cdot 12\text{H}_2\text{O}$ (FSW) (TC_{50} = 28.8 μM). FNSW also exerts a stronger inhibitory effect on HepG2 cells than 5-FU and FSW [8]. Rare earth elements change the cell membrane fluidity, permeability, ATP activity, intracellular and extracellular ion exchange, cell mitosis and DNA synthesis to affect the function of tumor tissues and cells [38]. Therefore, the rare earth element Nd could be used to improve the biological activity of POMs. In addition, $\text{K}_9(\text{C}_4\text{H}_4\text{FN}_2\text{O}_2)_2\text{Nd}(\text{PW}_{11}\text{O}_{39})_2\cdot 25\text{H}_2\text{O}$ (FNdPW) is a chemically synthesized drug that contains synthesized rare earth elements, which have low cytotoxicity. FNdPW significantly decreases the viability of A549 cell line and induces apoptosis by inducing significant activation of caspase 3-dependent signaling pathways [39]. Separately, the POM-BP complex $\text{Mo}_4\text{Zol}_2\text{Mn}^{\text{III}}$ has been studied in a mouse xenograft model bearing human Ewing sarcoma cell line (SK-ES-1), which revealed good results. The experiments showed that the POM-BP complex does not reduce the weight of the mice, indicating that the complex exhibits low toxicity to the body [20].

A cytotoxicity study using noncancerous breast epithelial cells (MCF-10A) and breast cancer cells (MCF-7 and MDA-MB-231) have shown that POM-biomolecule conjugates derived from the conjugation of a Tris-modified POM cluster (Tris-POM-Tris) (Tris: Tris(hydroxymethyl)aminomethane) with certain organic molecular forms of CA-POM-CA (CA: cholic acid) and DHCA-POM-DHCA

(DHCA: dehydrocholic acid) exhibit improved bioactivity and induce reduced side effects. These novel POM-biomolecule hybrid compounds exert potential synergistic effects and lower cytotoxicity (Table S1) [40]. In addition, glycine-functionalized POMs $(\text{K}_2\text{Na}[\text{As}^{\text{III}}\text{Mo}_6\text{O}_{21}(\text{O}_2\text{CCH}_2\text{NH}_3)_3]6\text{H}_2\text{O})$ exhibit lower toxicity to normal cells (human umbilical vein endothelial cell line, HUVECs) and better antiproliferative effects in vitro [41, 42]. In addition, Wang et al. designed and synthesized a new POM complex with a sandwich structure $[\text{Na}(\text{H}_2\text{O})_4][\{\text{Na}_3(\text{H}_2\text{O})_5\}\{\text{Mn}_3(\text{bpp})_3\}(\text{SbW}_9\text{O}_{33})_2]\cdot 8\text{H}_2\text{O}$ (MnSbW-bpp, bpp = 1,3-bis(4-pyridyl) propane) based on a flexible ligand. In addition, the IC_{50} values of MnSbW-bpp to normal human kidney inherent cell line (HMC) are 33.5 μM , whereas the IC_{50} values to other cancer cells are almost always below 10 μM , which indicates that MnSbW-bpp is more toxic to cancer cells than normal cells (Table S1) [43].

Application of novel POM nanocomposites

POMs have a special and complex architecture with dimensions up to the nanoscale. Natural or synthetic biopolymers, as nanocarriers for a variety of drugs, can enhance drug stability and help maintain the biological activity of drugs with decreased side effects through encapsulation [44]. The choice of carrier material has an important influence on the pharmacokinetics of nanodrugs [45]. The pharmacokinetics and pharmacodynamics of a series of POMs can be improved by conjugation with carriers, and the toxicity of POM-based nanocomposites is lower than that of POMs alone.

Chitosan is a linear polysaccharide derived from the deacetylation of chitin, a process that forms natural metabolites in organisms. Chitosan is nontoxic and can be completely absorbed by organisms, which indicates its great advantages as an agent for the sustained release of drugs [46]. POMs have been observed to be toxic only at very high doses, but at concentrations below 0.01 mg/ml, no significant signs of cell death are detected among human oral epidermoid cancer cell line (KB), MCF-7 cell line, human prostate cancer cell line (PC-3), or A549 cell line. However, the chitosan/EuWA (EuWA: $[\text{Cs}\subset\text{Eu}_6\text{As}_6\text{W}_{63}\text{O}_{218}(\text{H}_2\text{O})_{14}(\text{OH})_4]^{25-}$) nano-complex is highly toxic to cancer cells even at a dose of 7 $\mu\text{g}/\text{mL}$ [47]. This complex is a good example of enhanced toxicity caused by nanoencapsulation. Both carboxymethyl chitosan (CMC) and trimethyl chitosan (TMC) are ideal drug carriers for the encapsulation of intact bioactive POMs. Marked differences in the uptake by HeLa cells are found between POM-CMC (POM: $\text{K}_6\text{H}_2[\text{CoW}_{11}\text{TiO}_{40}]\cdot 13\text{H}_2\text{O}$ ($\{\text{CoW}_{11}\text{TiO}_{40}\}$)) and POM-TMC nanoparticles. TMC, as a stabilizer of $\text{CoW}_{11}\text{TiO}_{40}$, can transport POMs, improve their selectivity and reduce their toxic effects on normal cells and tissues [48, 49]. In addition, Pérez-Álvarez et al. reported

that Wells–Dawson-type $[P_2Mo_{18}O_{62}]^{6-}$ phosphomolybdate can be loaded into covalently crosslinked chitosan nanogels that can act as nanocarriers for local delivery [50]. Their work showed that selected chitosan nanocarriers have great potential for the delivery of POMs into tumor cells due to their pH-triggered delivery ability, which inhibits the release of cytotoxic drugs at physiological pH.

The compound chitosan- $[NaP_5W_{30}O_{110}]^{14-}$ (CTS- P_5W_{30}) also shows higher cytotoxicity than the standard anticancer drug vincristine along with minimal toxicity to normal cells [Vero cells, a cell line derived from the kidney of the African green (vervet) monkey]. The percent inhibition obtained with 10 μ M CTS- P_5W_{30} against HeLa cells and Vero cells is 7–12% and 78–98%, respectively. The cytotoxic behavior of chitosan-encapsulated POMs differs from that of nonencapsulated POMs [16]. The low-molecular-weight carbohydrate polymer nanocomposites CSYC100 and $CoW_{11}CpTi$ show lower toxicity to the C2C12 (normal murine/mouse myoblast cell line) and A549 cell lines. The finding that 95% of the total C2C12 cells remained viable after the experiment indicate that the nanocomposites at a concentration of 1.25 mM exert no toxic effects on C2C12 cells. In contrast, 5 mM bare $CoW_{11}CpTi$ is toxic to A549 cancer cells. Encapsulation increase the viability of the cells from 10 to 55%. $CoW_{11}CpTi$ in complex with CSYC100 can significantly reduce the toxic effects on C2C12 mouse myoblast cells [51]. The encapsulation of POMs makes them more target-oriented with minimal side effects. In 2018, Zamolo et al. synthesized $(nBu_4N)_3H[\gamma-SiW_{10}O_{36}\{(C_5H_7N_2O_5)(CH_2)_4 CONH(CH_2)_3Si\}_2O]$ (TBA-POM-biot₂), and cell imaging verified that it targets HeLa cells [52]. In 2019, Pérez-Álvarez et al. prepared chitosan nanogels as delivery nanocarriers for the loading of Wells–Dawson-type $[P_2Mo_{18}O_{62}]^{6-}$ phosphomolybdate. The nanogels have excellent properties, including low toxicity and ease of absorption and metabolism [50].

Microspheres such as starch microspheres and liposomes are ideal drug carriers with excellent biocompatibility, biodegradability and physical stability, which can reduce the side effects and incompatibility of drugs [53]. In 2003, Liu et al. reported the antitumoral activity and toxicity of starch-loaded $K_6H_2[CoW_{11}TiO_{40}] \cdot 12H_2O$ ($CoW_{11}Ti$)₁₃ nanoparticles. A cellular toxicity test has shown that $CoW_{11}Ti$ encapsulated by starch is less toxic in vitro than its parent $CoW_{11}Ti$ [17]. Starch-loaded $\alpha-K_8H_6[Si_2W_{18}Ti_6O_{77}]$ ($Si_2W_{18}Ti_6$) also exhibits significant advantages after encapsulation by starch. A comparison of LD₅₀ results indicates that the acute toxicity of $Si_2W_{18}Ti_6$ /starch is lower than that of pure POM, and the underlying mechanism is that the starch microspheres may prolong the residence time of the POMs by improving their stability and inhibiting their decomposition into toxic molecules. These three effects observed with starch decrease the

toxicity of $Si_2W_{18}Ti_6$. Moreover, in vivo experiments have shown that $Si_2W_{18}Ti_6$ /starch exerts no significant effect on the growth of rat fetuses, and the toxicity to rat fetuses is weak. This complex shows higher antitumor activity and lower toxicity in in vitro and in vivo experiments and no teratogenicity to pregnant rats [54].

In recent years, studies have extensively researched the development of liposomes as drug delivery carriers. The analysis of liposome-encapsulated polyoxometalate (LEP) nanoparticles containing $K_6[SiW_{11}TiO_{40}] \cdot 16H_2O$ ($SiW_{11}Ti$) has shown that liposomes exert no killing effect on HUVECs, whereas LEPs have reduced side effects compared with $SiW_{11}Ti$. The toxicity of POMs to normal cells is reduced due to the protective effects of the lipids. The LD₅₀ of $SiW_{11}Ti$ LEP in mice is 2003 mg/kg (95% CI 1856–2374 mg/kg). An LD₅₀-based comparison between LEPs and POMs (LD₅₀ of $SiW_{11}Ti$ = 394 mg/kg) indicates that liposome encapsulation reduces the acute toxicity of POMs [55]. Additionally, Razavi et al. synthesized nanolipid-loaded Preyssler (NLP, Preyssler: $H_{14}[NaP_5W_{30}O_{110}]$) and studied its antitumor activity against HepG2 cells [56]. The IC₅₀ value of the loaded nanoliposomes for normal cells [primary human foreskin fibroblasts (HFFs)] was found to equal 2000 μ g/mL at 72 h, which is markedly better than that of sorafenib (16 μ g/mL). The entrapment efficiency of nanoliposomes reaches 53.8%, which clearly reduces the toxicity of Preyssler.

A novel platinum (IV)-substituted Keggin-type POM prodrug $[PW_{11}O_{40}(SiC_3H_6NH_2)_2Pt(NH_3)_2Cl_2]^{3-}$ (Pt^{IV} - PW_{11}) has been designed. Compared with classic cisplatin, PW_{11} and Pt^{IV} - PW_{11} exert better inhibitory effects on the growth of HT29 cells (human colorectal cancer cell lines). Researchers then encapsulated Pt^{IV} - PW_{11} with 1,2-distearoyl-*sn*-glycero-3-phosphoethanolamine-*N*-[methoxy (polyethylene glycol)-2000] (DSPE-PEG2000) to form Pt^{IV} - PW_{11} -DSPE-PEG2000 nanoparticles (Pt^{IV} - PW_{11} -DSPE-PEG2000 NPs). DSPE-PEG2000 NPs exhibit improved cellular targeting in acidic microenvironments, which decreases drug release under high pH conditions and the accumulation in the kidney. Pt^{IV} - PW_{11} -DSPE-PEG2000 exhibit lower cytotoxicity against HUVECs cell line and fewer side effects on mice than cisplatin [15]. The Kabanos-type POM $[Na\{(Mo_2^VO_4)_3(\mu_2-O)_3-(\mu_2-SO_3)_3(\mu_6-SO_3)_2\}]^{15-21}$ has been modified with gold nanoparticles (AuNPs) to form AuNPs@POM. The results show that AuNPs@POM exerts greater antiproliferative effects on mouse melanoma cell line (B16) than on Vero cells. In other words, AuNPs@POM exhibits lower toxicity to normal cells [57]. In addition, Tang et al. used hollow mesoporous organosilica nanoparticles (HMOPs) to encapsulate $Mn_2(CO)_{10}$ (Mo(VI)-based POM clusters), which resulted in the formation of more stable $Mn_2(CO)_{10}$ @HMOPs (HMOPs-CO). To assess the toxicity of HMOPs-CO and HMOPs, these researchers performed blood index tests, a major organ histological

analysis and evaluation of weight changes in BALB/c mice (10 mg Mo/kg). All the results suggest that both HMOPMs-CO and HMOPMs exhibit low toxicity in vivo [58].

Interestingly, Zhou J et al. synthesized monodisperse renal-clearable W-based POM nanoclusters (W-POM NCs; average diameter of approximately 2.0 nm) [59]. The as-prepared W-POM NCs show biocompatibility toward normal cells/tissues both in vitro and in vivo because no obvious toxicity was observed over a 30-day period after the treatment of female BALB/c mice with concentrated W-POM NCs. More importantly, W-POM NCs exhibit not only better near-infrared (NIR) light absorption (a coloration effect originating from the existence of electron-trapped W^{5+}) for efficient tumor photothermal therapy but also impressive anti-inflammatory ability (eliminating inflammation-related ROS by the oxidation of W^{5+} into the W^{6+} state) to obtain better therapeutic outcomes. Thus, these W-POM NCs are safe and efficient. In 2021, Isakovic AM et al. reported a molecular noble metal-oxo nanoclusters, $Na_8[Pd_{13}As_8O_{34}(OH)_6] \cdot 42H_2O$ (Pd_{13}) [60]. Pd_{13} had excellent antitumor potential against human neuroblastoma cell line (SH-SY5Y). The obtained IC_{50} values for 24 h and 48 h treatment with Pd_{13} were $7.2 \pm 2.2 \mu M$ and $4.4 \pm 1.2 \mu M$, respectively. The molecular mechanisms of Pd_{13} -induced antitumor action include apoptotic cell death and autophagy induction. Because of a good metabolic stability, Pd_{13} cannot act cytogenotoxic to the healthy human peripheral blood cell line (HPBCs) at 25 μM (25 $\mu M \approx 3 \times IC_{50}$ (24 h) for SH-SY5Y). Additionally, Zheng et al. constructed a novel supramolecular nanocage $((NH_2Me_2)_{12}[(V_5O_9Cl)_6(tatb)_8])$, VMOP-31. VMOP-31 has been applied to hepatic tumors both in vitro and in vivo. The researchers used human normal bronchial epithelial cell line (BEAS-2B) to study the cytotoxicity of VMOP-31. The obtained IC_{50} values are markedly lower than those in SMMC-7721, MCF-7, and A549 cell lines, which indicates that VMOP-31 is selectively toxic toward solid tumor cells over normal cells [61]. In addition, peptides can also serve as excellent ligands. As a result, this novel biohybrid could decrease the on-POM folding of the chains and has no tendency to self-assemble into spherical vesicles. The compound $([MnMo_6O_{18}\{(OCH_2)_3CNHCO(CH_2)_2CO(Ttds-EEEE\beta A-fQWAVGHL-NHEt)\}_2])_3$ displays IC_{50} values in the range of 10–100 mM [62].

Overall, the encapsulation of bioactive POMs into a biopolymer is a new method for the medical application of these promising drug prototypes and for the development of new composites with functionalized hybrid POMs or specially designed polymers.

Application of POMs for anti-infection therapy

POMs have been shown to be active against a variety of DNA and RNA viruses, including influenza viruses A and B, HBV, hepatitis C virus (HCV), herpes simplex virus, dengue virus and HIV [8, 38–41]. In addition, POMs play an important role in antibacterial activity.

Application of POMs for anti-HIV therapy

According to the 2019 United Nations Joint Program of HIV/acquired immunodeficiency syndrome (AIDS) report, 37.9 million people worldwide are living with HIV, and approximately 1.7 million people are newly infected [63]. HIV remains the main threat to public health worldwide. Currently, combination antiretroviral therapy comprises three or four types of anti-HIV-1 drugs that work against agents during multiple stages of the HIV-1 life cycle, including viral reverse transcriptase, integrase, protease, and viral invasion and fusion. Despite great success, drug resistance and side effects cannot be ignored [3, 64].

HPA-23 was the first POM to be used in clinical trials of AIDS but failed due to its unacceptable adverse effects [3, 64]. Since then, several groups have focused on the synthesis of new derivatives of POMs, which not only make POMs less toxic but also increase their antiviral activity in most cases.

In recent years, the anti-HIV activity of POMs has attracted attention. However, the application of POMs for HIV therapy remains in its infancy, and the toxicity and side effects of POMs have rarely been evaluated. Craig L. et al. studied the anti-HIV activity and toxicity of six structural categories of POMs in human peripheral blood mononuclear cells (PBMC), including HPA-23, $X^n + W_{12}O_{40}^{(8-n)-}$ (Keggin), $P_2W_{18}O_{62}^{6-}$ (Wells–Dawson), $W_6O_{19}^{2-}$ (Lindqvist), $[NaP_6W_{30}O_{110}]^{14-}$ (Preyssler), and $W_{10}O_{32}^{4-}$ (decatungstate) [65]. Studies have shown that compounds containing fewer than eight metal ions, such as $(n-Bu_4N)_2W_6O_{19}$, $(n-Bu_4N)_2Mo_6O_{19}$, $a-(n-Bu_4N)_2Mo_8O_{26}$, and $K_4W_4O_{10}(O_2)_6$ (all median effective concentration (EC_{50}) values $> 50 \mu M$), have low antiviral activity. However, the anti-HIV activity of the remaining compounds, including the compounds $H_4SiW_{12}O_{40}$, $Na_6H_2W_{12}O_{40}$, and $K_8SiW_{11}O_{39}$, is equal to or higher than that of HPA-23. The EC_{50} value of HPA-23 is 0.39 μM . Most polyoxometalates have low toxicity to PBMC, and their IC_{50} values are lower than that of HPA-23 [65].

As mentioned previously, POMs are unstable under physiological pH conditions (the blood serum pH value is generally 7.4) [17, 22, 55, 66], which limits the development of antiviral POMs. Heteropolytungstates of the Wells–Dawson

class containing hydrolytically stable Nb were synthesized by Deborah A Judd et al. The new compounds ($\alpha 1$ -K₇[P₂W₁₇(NbO₂) O₆₁] ($\alpha 1$ 1), $\alpha 2$ -K_{6.7}H_{0.3}[P₂W₁₇(NbO₂) O₆₁] ($\alpha 2$ 1), $\alpha 1$ -K_{6.9}Li_{0.1}[P₂W₁₇NbO₆₂], ($\alpha 1$ 2), and $\alpha 2$ -K₇[P₂W₁₇NbO₆₂] ($\alpha 2$ 2)) are active against HIV-1 and selectively inhibit HIV protease, as evaluated in HIV-1-infected PBMC. These researchers solved the instability problem of POMs (they were stable at pH 7), and the research showed that they all exhibit high inhibitory activity against HIV-1 protease (EC₅₀: 0.17–0.83 μ M) and minimal toxicity (IC₅₀: 50 to > 100 μ M) [66]. Keggin polyoxotungstate K₇(PTi₂W₁₀O₄₀)·6H₂O (PM-19) [3, 67] not only functions as an anti-HIV agent but also acts against herpes simplex virus (HSV) [67–69]. PM-19 can inhibit the interaction between the HSV envelope protein (gD, glycosylated ectodomain) and cell surface membrane proteins to perform its anti-HSV functions [70]. Additionally, PM-19 is less toxic and more efficient than HPA-23. Recently, Wang et al. introduced an organic amine into the PM-19 structure [K₇(PTi₂W₁₀O₄₀)] and synthesized a series of novel pyridinium polyoxometalates (A₇PTi₂W₁₀O₄₀). Their studies showed that the introduction of the organic amine improves the stability of the compounds and reduces the cytotoxicity compared with that of the original compounds. The TD₅₀ value of PM-19 is 9.34 ± 0.32 μ M, whereas the TD₅₀ values of the remaining compounds are greater than 25 μ M. [3]. Another Keggin polyoxometalate with low cytotoxicity and genotoxicity, PT-1 (K₆HPTi₂W₁₀O₄₀), also efficiently interferes with HIV reverse transcriptase and integrase by blocking the gp120-binding site of the CD4 receptor and interacting with the gp41 NHR (N36 peptide) to prohibit the entry of the virus [64]. To better understand the toxicity of POMs with different structures, we summarized their toxicity in anti-HIV therapy in Table S2.

From this point of view, the introduction of new elements makes the newly developed POMs not only more stable and less toxic than the original compounds but also plays an important role in anti-HIV treatment.

Application of POMs for anti-HBV/HCV therapy

POMs are also potential candidates for anti-HBV and HCV therapy [4, 19, 71]. For example, Cs₂K₄Na [SiW₉Nb₃O₄₀]·H₂O (POM93) can inhibit the secretion and replication of HBV antigens in vitro in a dose- and time-dependent manner [72]. POM93 is located on the surface of cells rather than the interior and exhibits less cytotoxicity than the commercially available hepatitis B drug in HepG2 cells [71]. In addition, a study of its acute toxicity showed no abnormal changes after single doses up to 5000 mg/kg body weight in Wistar rats. An assessment of sub chronic toxicity in Wistar rats also showed that POM93 is safe for the respiratory, digestive, reproductive and other systems.

Compared with the untreated group, a histopathological analysis of various organs and their surrounding structures in the rats showed no inflammation, lesions or pathological changes after POM93 treatment [4]. The pharmacokinetics of POM93 indicates that the kidney and liver may be possible toxic sites [73]. Qi et al. administered POM93 to human HBV-transgenic mice at a dose of 6 × 10⁻⁵ mol/(kg day) for 28 days, which also proved that POM93 is safe and does not cause damage to liver tissue [72]. It can, therefore, be speculated that POM93 is safe for the human body and can serve as a highly effective anti-HBV drug. In addition, POM93 has a wide range of antiviral activities, such as activities against HIV, HSV, HCV and influenza A/influenza B [71].

As previously reported, POM-4, POM-6, and particularly POM-12 (Cs₂K₄Na [SiW₉Nb₃O₄₀]·H₂O) exhibit anti-HCV abilities. Yue Qi et al. [74] proposed that POM-12 can destroy the integrity of HCV by destroying the lipid layer of the viral envelope. A human lung cancer cell line (Huh7.5.1) viability study showed that the EC₅₀ and TC₅₀ values of POM-12 against HCV infection are 0.8 μ M and 119 μ M, respectively. A cytotoxicity assay with POM-12 indicated that it exerts no significant effect on Huh7.5.1-cell viability and can be used as a potential drug to protect individuals from hepatitis C virus infection in combination with ribavirin, a common drug used to treat HCV, or as a substitute for ribavirin. In addition to HCV, POM-12 also exerts an inhibitory effect on other flaviviruses, such as Dengue virus (DENV), Japanese encephalitis virus (JEV), and Zika virus (ZIKV). Studies have indicated that POM-12 can directly damage the integrity of these viruses and inhibit the replication of JEV at a post-entry step. The IC₅₀ values of POM-12 against DENV, JEV and ZIKV are 1.16 μ M, 1.9 μ M and 0.64 μ M, respectively. The TC₅₀ value of POM-12 is 149.1 μ M, which suggests that POM-12 does not suppress the virus by increasing cytotoxicity [75]. POM-12 exerts an effective inhibitory effect on flaviviruses, but its mechanism of action on different viruses is different and related to the surface topology and charge of virions. POM-12 may be modified to suppress these similar viruses.

In addition, the application of polyoxometalates for anti-HBV/HCV therapy is listed in Table S2.

Application of POMs for anti-influenza virus therapy

In recent years, influenza virus infection has remained a major threat to public health. As broad-spectrum drugs, POMs can protect against several respiratory viruses, including myxovirus, influenza virus, and coronaviruses, both in vitro and in vivo. Assessments of cytopathic effect inhibition and neutral red uptake assays have shown that HS-81 [Cs₄[(Cl(CH₂)₃Si)₂O]SiW₁₁O₃₉], HS-86 [(CH₃)₄N]₄[(CH₂ = CHSi)₂O]SiW₁₁O₃₉],

HS-106 $[(\text{Me}_3\text{NH})_8\text{Si}_2\text{W}_{18}\text{Nb}_6\text{O}_{77}\text{nH}_2\text{O}]$, and HS-116 $[(\text{LysineH})_7\text{KSi}_2\text{W}_{18}\text{Nb}_6\text{O}_{72}\text{18H}_2\text{O}]$, among others, exhibit significant anti-respiratory syncytial virus (RSV) inhibitory activities and low cytotoxicity to embryonic African green monkey kidney cell line (MA-104) and human larynx epidermoid carcinoma cell line (HEp-2). The IC_{50} values of these POMs range from 2 to 100 μM , and no difference has been found among the compounds against different types of RSV strains [4, 5, 9].

Keggin-type polyoxometalate PM523 $(\text{iPrNH}_3)_6\text{H}[\text{PTi}_2\text{W}_{10}\text{O}_{38}(\text{O}_2)_2]\cdot\text{H}_2\text{O}$ affects influenza virus (FluV) A, FluV B, RSV and the measles virus in vitro. PM523 is not markedly cytotoxic in canine kidney cells (MDCK), and the TC_{50} is lower than that of ribavirin [76]. PM-523 inhibits FluV A virus replication in MDCK cells by inhibiting fusion of the viral envelope and cell membrane [76–79]. The researchers found that PM523, when used in combination with ribavirin, is not only more effective against FluV activity but also less toxic to MDCK cells than either compound alone, as determined by the trypan blue exclusion method. Moreover, the combinations exert synergistic effects in mice infected with Flu-V A (H1N1). The combination of PM523 and ribavirin at a ratio of 1:16 resulted in a higher number of surviving mice than those obtained with either compound alone at the same dose and even twice the dose [77, 78].

Heteropolyoxometalates with Keggin-type structures are also inhibitors of FluV but are unstable at physiological pH, which limits their development. A new series of manganese-substituted mixed-valence rare earth borotungstate heteropolyoxometalates, $\text{Ln}_2\text{H}_3[\text{BW}_9^{\text{VI}}\text{W}_2^{\text{V}}\text{Mn}(\text{H}_2\text{O})\text{O}_{39}]\cdot 12\text{H}_2\text{O}$ (Ln (2)); Ln = La, Ce, Pr, Nd, Sm, Eu or Gd), as well as their corresponding heteropoly acids (Ln (0)), have been synthesized, and their effects against the influenza virus in MDCK cells have been investigated. Compared with archetype heteropolyacids, these newly synthesized compounds exhibit obvious thermal stability and acid–base stability. Most importantly, Ln (2) exhibits high activity against FluV A/B and less toxicity than Ln (0). The higher thermal stability of Ln (2) leads to slower decomposition and a moderate concentration of dissociated metal ions, such as Ln^{3+} and WO_4^{2-} , which results in its lower toxicity compared with that of Ln (0) [80]. Thus, POMs have been identified as promising first-line therapeutics against acute respiratory diseases and are characterized by their low toxicity and high efficiency. The application of polyoxometalates for influenza virus therapy is summarized in Table S2.

Application of POMs for antibacterial therapy

Polyoxometalates also play a crucial role as antibacterial agents because they exhibit both synergistic and direct antibacterial activity. A study found that

$\text{K}_6[\text{P}_2\text{W}_{18}\text{O}_{62}]\cdot 14\text{H}_2\text{O}$ (P_2W_{18}), $\text{K}_4[\text{SiMo}_{12}\text{O}_{40}]\cdot 3\text{H}_2\text{O}$ (SiMo_{12}), $\text{K}_7[\text{PTi}_2\text{W}_{10}\text{O}_{40}]\cdot 6\text{H}_2\text{O}$ ($\text{PTi}_2\text{W}_{10}$), and $\text{K}_9\text{H}_5[\alpha\text{-Ge}_2\text{Ti}_6\text{W}_{18}\text{O}_{77}]\cdot 16\text{H}_2\text{O}$ ($\text{Ge}_2\text{Ti}_6\text{W}_{18}$) enhance the antibacterial activity of β -lactams against methicillin-resistant *Staphylococcus aureus* (MRSA) and vancomycin-resistant *Staphylococcus aureus* (*S. aureus*, VRSA) [81, 82]. The mechanism underlying the inhibition by P_2W_{18} , SiMo_{12} , and $\text{PTi}_2\text{W}_{10}$ is associated with the inhibition of the transcription processes of the *mecA* and *pbp* genes into mRNA, but that of $\text{Ge}_2\text{Ti}_6\text{W}_{18}$ may be associated with the inhibition of a posttranscriptional process. The IC_{50} values of P_2W_{18} , SiMo_{12} , and $\text{PTi}_2\text{W}_{10}$ against Vero cells are 120 μM , 500 μM and 1000 μM , respectively [81]. Additionally, Keggin-type structural (hetero)polyoxotungstates with a lacunary hole, such as undecatungstosilicate $([\text{SiW}_{11}\text{O}_{39}])_8, \text{SiW}_{11}$, also improve the antibacterial activity of β -lactams against MRSA [83]. The polyoxotungstates $\text{K}_{27}[\text{KAs}_4\text{W}_{40}\text{O}_{140}]$ and $\text{K}_{18}[\text{KSb}_9\text{W}_{21}\text{O}_{86}]$, which are highly negatively charged, and Keggin-structural polyoxotungstates exhibit potent anti-*Helicobacter pylori* (*H. pylori*) activity. These polyoxotungstates can be taken up by *H. pylori* cells, the periplasmic space or the inner membrane to change the bacterial morphology into U-shaped or coccoid forms and subsequently induce bactericidal effects [84]. A study showed that polyoxotungstates, particularly those that are highly negatively charged against *H. pylori*, are stronger than polyoxomolybdates [84]. The newly generated organoantimony (III)-containing heteropolytungstates, such as $[(\text{PhSb}^{\text{III}})_4(\text{A}\text{-}\alpha\text{-GeIVW}_9\text{O}_{34})_2]^{12-}$, $[(\text{PhSb}^{\text{III}})_4(\text{A}\text{-}\alpha\text{-PVW}_9\text{O}_{34})_2]^{10-}$, and $[\{2\text{-}(\text{Me}_2\text{NCH}_2\text{C}_6\text{H}_4)\text{Sb}^{\text{III}}\}_3(\text{B}\text{-}\alpha\text{-As}^{\text{III}}\text{W}_9\text{O}_{33})]^{3-}$, $\text{Na}\{2\text{-}(\text{Me}_2\text{HN}^+\text{CH}_2)\text{C}_6\text{H}_4\text{Sb}^{\text{III}}\}\text{As}^{\text{III}}_2\text{W}_{19}\text{O}_{67}(\text{H}_2\text{O})]^{10-}$, $[\{2\text{-}(\text{Me}_2\text{HN}^+\text{CH}_2)\text{C}_6\text{H}_4\text{Sb}^{\text{III}}\}_2\text{As}^{\text{III}}_2\text{W}_{19}\text{O}_{67}(\text{H}_2\text{O})]^{8-}$, and $[\{2\text{-}(\text{Me}_2\text{HN}^+\text{CH}_2)\text{-C}_6\text{H}_4\text{Sb}^{\text{III}}\}\{\text{WO}_2(\text{H}_2\text{O})\}\{\text{WO}(\text{H}_2\text{O})\}_2(\text{B}\text{-}\beta\text{-As}^{\text{III}}\text{W}_8\text{O}_{30})(\text{B}\text{-}\alpha\text{-As}^{\text{III}}\text{W}_9\text{O}_{33})_2]^{14-}$ inhibit the growth of different Gram-positive and Gram-negative bacteria, and their bioactivity can be tuned by controlling the number and type of introduced organoantimony(III) groups [85, 86]. The novel decavanadate cluster complex $[\text{H}_2\text{V}_{10}\text{O}_{28}][4\text{-picH}]_4\cdot 2\text{H}_2\text{O}$ exerts antimicrobial effects against Gram-positive and Gram-negative bacteria as well as fungi in vitro. Comet and plasmid nicking assays have demonstrated that the complex causes negligible damage to DNA and an inappreciable amount of cytotoxic damage compared with the similar sodium decavanadate salt $\text{Na}_6[\text{H}_2\text{V}_{10}\text{O}_{28}]\cdot 18\text{H}_2\text{O}$ [87]. Thus, this new complex may become a new antimicrobial agent. Chitosan has good biocompatibility, and composite films with antibacterial activity can be prepared by encapsulating POM with chitosan. For example, G. F et al. encapsulated POMs $(\text{NH}_4)_6\text{V}_{10}\text{O}_{28}$ (V_{10}), $\text{H}_5\text{PMo}_{10}\text{V}_2\text{O}_{40}$ (Mo_{10}V_2), and $\text{Na}_4\text{W}_{10}\text{O}_{32}$ (W^{10}) in chitosan and synthesized a series of novel nanocomposites that exhibit improved cell penetration and better antibacterial ability [88].

In addition, POMs are excellent carriers and stabilizers for antibacterial agents. Based on the activity of polyoxometalates ($\text{Ag}_3\text{PW}_{12}\text{O}_{40} = \text{AgPW}$) against Gram-positive bacteria, a new type of composite material, $\text{AgPW}@ \text{PDA}@ \text{Nisin}$, which has a shell-core structure, was successfully synthesized using conjugated nisin on the surface of polydopamine as the shell and AgPW as the core [89]. This newly synthesized material can destroy the cytoplasmic membrane of *S. aureus*, change its permeability and induce its death. The minimum inhibitory concentration (MIC) and minimum bactericidal concentration (MBC) were found to equal 4 and 32 $\mu\text{g}/\text{mL}$, respectively. An MTT assay was performed to determine the effects of $\text{AgPW}@ \text{PDA}@ \text{Nisin}$ on human dermal fibroblasts (HDF- α), and the results indicated that nanoflowers exhibit low cytotoxicity. Ag^+ is an effective antibacterial agent that can interact with proteins and cell structures to destroy the physiological functions of bacteria. A silver-encapsulated Preyssler-type POM, $[\text{AgP}_5\text{W}_{30}\text{O}_{110}]^{14-}$ ($\text{AgP}_5\text{W}_{30}$), reportedly exhibits antibacterial activity by continuously releasing Ag^+ in exchange with Na^+ [90]. The new materials synthesized by combining POMs with other antibacterial agents can greatly improve the antibacterial activity and reduce the cytotoxicity of POMs, and this method provides a new idea for the development of antibacterial materials.

Hemant K. Daima et al. functionalized tyrosine-reduced AuNPs (AuNPsTyr) [91] and tyrosine-reduced AgNPs (AgNPsY) using two different POMs, 12-phosphoric acid (PTA) and 12-phosphomolybdic acid (PMA). The introduction of POMs increases the activity of the nanomaterials against the Gram-negative bacterium *Escherichia coli*. The introduction of AuNPsTyr also increases the activity against A549 cells [92]. Most importantly, none of the nanoparticles, including AgNPsY , $\text{AgNPsY}@ \text{PMA}$, and $\text{AgNPsY}@ \text{PTA}$, show nontoxicity in human PC-3 cells. These studies indicate that the surface corona of POMs exerts a strong effect on the toxicity and biological applicability of nanomaterials. In addition, the introduction of POMs has increased the use of nanomaterials in the field of antimicrobials. Because POMs are only located on the periphery of bacterial cells, future studies should attempt to identify potential targets of extracellular or membrane-related proteins to elucidate the interaction mechanism between POMs and bacterial cells and improve the targeting properties of POM-based nanocomposites [93].

POMs as inhibitors of amyloid β peptide aggregation for the treatment of Alzheimer's disease

AD is a degenerative disease of the central nervous system characterized by extracellular amyloid plaques and intracellular neurofibrillary tangles [12, 94]. According to the latest research results, aggregation of the amyloid β peptide ($A\beta$) into amyloid fibrils and the generation of excessive ROS are two essential mechanisms of AD pathogenesis. Recent advances have demonstrated that polyoxometalates are inhibitors of $A\beta$ aggregation in the treatment of AD [12, 94–98]. POM- $\text{K}_8[\text{P}_2\text{CoW}_{17}\text{O}_{61}]$, which has a Wells–Dawson structure, can inhibit $A\beta$ fibril formation. Furthermore, the recognition of $A\beta$ and amyloid inhibition may be correlated with the size of the POM, whereas selective inhibition may be related to the specific electrostatic interaction between the POM and $A\beta$. Studies have shown that while the smaller Anderson compound has no activity, the larger Keggin compound has moderate activity, and the largest Dawson compound exhibits the highest inhibitory activity. POMs might bind to the His13 to Lys16 (HHQK) cationic cluster of $A\beta$ to interfere with fibril formation. In addition, studies have shown that transition metal (such as Ni(II)-, Co(II)- or Pt(II)-) functionalized POM derivatives with specific histidine chelating sites have better anti- $A\beta$ activity and peroxide inhibitory activity than the parental POM. These compounds can pass although the blood–brain barrier (BBB) and be metabolized after 48 h [94, 99].

Based on the interference of $A\beta$ fibril formation, researchers have combined $\text{K}_8[\text{P}_2\text{CoW}_{17}\text{O}_{61}]$ with the well-known $A\beta$ targeting peptide inhibitor $A\beta_{15-20}$ (Ac-QKLVFF-NH_2) for self-assembly [95] and combined the unique high NIR absorption properties of gold nanorods with these two $A\beta$ inhibitors [96]. These final compounds display stronger targeting abilities than the parent POMs, inhibit amyloid aggregation in the cerebrospinal fluid of mice and protect cells from $A\beta$ -related toxic effects. The PC12 has been used to probe cellular metabolism using the MTT assay. The results show that POMs could significantly improve the cell survival rate, inhibit $A\beta$ aggregation and reduce the cytotoxicity induced by $A\beta$ [95, 96]. Similarly, peptide-modified Mo-POM nanoparticles have been synthesized by the self-assembly of $A\beta$ target peptides and Mo-POMs [100]. The Peptide@Mo-POMs suppress $A\beta$ aggregation, disaggregate $A\beta$ fibrils, and suppress Zn^{2+} -induced $A\beta$ aggregation. These results provide new ideas for the design and synthesis of Peptide@POMs as $A\beta$ inhibitors in the treatment of AD.

In addition, Ma M et al. developed a redox-activated NIR responsive POM-based nanoplatform ($\text{rPOMs}@ \text{MSNs}@ \text{copolymer}$), which can not only hinder $A\beta$ aggregation but also serve as a reducing agent to clean superfluous ROS

[101]. The nanoplatform consists of mesoporous silica nanoparticles (MSNs), reduced POMs (rPOMs), and the thermally responsive copolymer poly(N-isopropylacrylamide-co-acrylamide). The coinubation of PC12 cells with A β monomer for 48 h increased the ROS levels (174.35%) compared with those found in the untreated group, whereas the ROS levels are significantly decreased to 52.81% after coinubation with rPOMs@MSNs@copolymer under near-infrared laser irradiation. The MTT test showed that rPOMs@MSNs@copolymer could significantly improve the cell viability (92.6%) of PC12 cells after coinubation with A β monomer for 48 h. This material provides a new method for using rPOMs for the NIR photothermal treatment of AD.

In addition, acetylcholinesterase (AChE), an enzyme responsible for the hydrolysis of the neurotransmitter acetylcholine, helps with the formation of β -amyloid. AChE inhibitors such as donepezil, rivastigmine, and galantamine are important in the treatment of neurodegenerative diseases. Recent data in the literature show that POMs can act as inhibitors of AChE, which makes them potential anti-AD drugs. Mirjana B et al. selected two Keggin-type heteropolytungstates, $K_7[Ti_2PW_{10}O_{40}] \cdot 6H_2O$ (K-Ti₂PW₁₀) and $K_6H[SiV_3W_9O_{40}] \cdot 3H_2O$ (K-SiV₃W₉), with different inhibitory potencies toward AChE activity (IC₅₀ values of 1.04 μ M and 480 μ M, respectively) to study their toxicity. The in vivo studies have shown that neither POM type can be considered highly toxic. Because there was no influence on the rat body mass and food intake. However, a histopathological analysis showed that K-SiV₃W₉ could induce reversible liver tissue damage [102]. The IC₅₀ values of the compounds $[H_2W_{12}O_{42}]^{10-}$ and $[TeW_6O_{24}]^{6-}$ are 0.29 ± 0.01 and 0.31 ± 0.01 μ M, respectively [103]. 12-Tungstosilicic acid (WSiA) and 12-tungstophosphoric acid (WPA) have been shown to inhibit AChE activity at nanomolar concentrations. Studies have shown that these two POMs with Keggin-type structures exhibit no genotoxicity or cytotoxicity but can induce mild inhibition of cell growth in a concentration-dependent manner. Furthermore, WSiA and WPA can interact with the β -allosteric site in AChE, and this binding may prevent the conversion of the AChE586-599 region from the α -helical to the β -strand and thereby inhibits the AChE-associated aggregation of amyloid- β pmmc1, which plays a key role in the pathogenesis of AD [104].

It is believed that the application of POMs may contribute to the development of new multifunctional AD therapeutic materials. The application of polyoxometalates for AD therapy is summarized in Table S3.

Summary and outlook

POMs and POM-based hybrid compounds have great potential as antitumor, antiviral (anti-HIV, anti-HBV and so on), antibacterial and anti-AD agents. However, the application of POMs is limited by some drawbacks, including high toxicity and thermodynamic and kinetic instability under physiological conditions [17, 94]. At present, the clinical development of POMs remains in its infancy, and researchers are still developing derivatives of POMs with low toxicity, high stability, and good biological activity to obtain superior antitumor, anti-infection and anti-AD effects. Novel POM-based molecular and composite materials are the focus of current research. The conjugation of organic molecules or bioactive transition metals onto the POM core or skeleton can reduce the POM toxicity. In addition, POM conjugates/encapsulates in some biopolymeric delivery vehicles can significantly reduce the toxicity caused by metal ions and improve their biocompatibility. For example, POMs can be effectively used in sustained-release drug delivery systems by embedding the POMs into nontoxic chitosan and other drug carriers with high biocompatibility, which can enhance their stability at physiological pH. In addition, the incorporation of POMs into nanocomposites can significantly improve their biocompatibility and reduce their toxicity and instability. Furthermore, anticancer, anti-infection and anti-AD drugs can be doped into POM-based nanocomposites to further improve their biological properties. The biological and pharmacokinetic properties of POM-based nanocomposites appear to be superior to those of organically functionalized POMs. The development of more POM-based nanocomposites for anticancer, anti-infection and anti-AD therapy is the focus of future research.

Some possible toxicity mechanisms of POMs have been proposed, and these include competing with acetylated low-density lipoprotein (LDL) for the scavenger receptor of macrophages [95], binding to proteins through electrostatic interactions, tending to be deposited in organs in the body with abundant blood flow, such as the liver, spleen, lungs and kidneys [4], and not being easily excreted by the body [28]. Although possible mechanisms have been proposed, the specific mechanism underlying the action of POMs on cells and the body has not been determined. Future research will focus on the design and synthesis of novel POM hybrids, which currently exhibit excellent toxicity, pharmacokinetic properties, and biological activity. Furthermore, eliminating the toxicity mechanisms of POMs and reducing their high toxicity will open a new avenue for making POMs the next generation of drugs against tumors, viral infections, bacterial infections, and AD.

Supplementary Information The online version contains supplementary material available at <https://doi.org/10.1007/s00775-022-01942-7>.

Acknowledgements The authors thank the National Natural Science Foundation of China (Grant No. 82073557, 82073603, and 81872668), the Education Department of Jilin Province (Grant No. JJKH20221100KJ) and the Fundamental Research Funds for the Central Universities (45121031D060) for the financial support provided.

Declarations

Conflict of interest The authors declare that they have no conflicts of interest.

References

- Shigeta S et al (2003) Broad spectrum anti-RNA virus activities of titanium and vanadium substituted polyoxotungstates. *Antivir Res* 58(3):265–271
- Lee S-Y et al (2015) Polyoxometalates—potent and selective ecto-nucleotidase inhibitors. *Biochem Pharmacol* 93(2):171–181
- Wang S et al (2017) Synthesis and evaluation of pyridinium polyoxometalates as anti-HIV-1 agents. *Bioorg Med Chem Lett* 27(11):2357–2359
- Qu X et al (2017) Genotoxicity and acute and subchronic toxicity studies of a bioactive polyoxometalate in Wistar rats. *BMC Pharmacol Toxicol* 18(1):26
- Bijelic A, Aureliano M, Rompel A (2019) Polyoxometalates as potential next-generation metallodrugs in the combat against cancer. *Angew Chem Int Ed Engl* 58(10):2980–2999
- Arefian M et al (2017) A survey of the different roles of polyoxometalates in their interaction with amino acids, peptides and proteins. *Dalton Trans* 46(21):6812–6829
- Ueda T (2021) Polyoxometalates in analytical sciences. *Anal Sci* 37(1):107–118
- Liu X, Wang S (2010) Synthesis and anticancer properties of tungstosilicic polyoxometalate containing 5-fluorouracil and neodymium. *J Rare Earths* 28(6):965–968
- Barnard DL et al (1997) Potent inhibition of respiratory syncytial virus by polyoxometalates of several structural classes. *Antivir Res* 34(1):27–37
- Shigeta S et al (1995) In vitro antimyxovirus and anti-human immunodeficiency virus activities of polyoxometalates. *Antivir Chem Chemother* 6(2):114–122
- Shahid M et al (2014) Isolation of a decavanadate cluster [H₂V₁₀O₂₈][4-picH]4·2H₂O (4-pic). *J Cluster Sci* 25(5):1435–1447
- Geng J et al (2011) Polyoxometalates as inhibitors of the aggregation of amyloid β peptides associated with Alzheimer's disease. *Angew Chem Int Ed* 50(18):4184–4188
- Ogata A et al (2005) A novel anti-tumor agent, polyoxomolybdate induces apoptotic cell death in AsPC-1 human pancreatic cancer cells. *Biomed Pharmacother* 59(5):244
- Yanagie H et al (2006) Anticancer activity of polyoxomolybdate. *Biomed Pharmacother* 60(7):349–352
- Sun T et al (2016) Target delivery of a novel antitumor organoplatinum(IV)-substituted polyoxometalate complex for safer and more effective colorectal cancer therapy in vivo. *Adv Mater* 28(34):7397–7404
- Shah HS et al (2014) Cytotoxicity and enzyme inhibition studies of polyoxometalates and their chitosan nanoassemblies. *Toxicol Rep* 1:341–352
- Wang X, Liu J, Pope MT (2003) New polyoxometalate/starch nanomaterial: synthesis, characterization and antitumoral activity. *Dalton Trans* 5:957–960
- León IE et al (2014) Polyoxometalates as antitumor agents: bioactivity of a new polyoxometalate with copper on a human osteosarcoma model. *Chemico Biol Interact* 222:87–96
- Wang X et al (2003) Synthesis and antitumor activity of cyclopentadienyltitanium substituted polyoxotungstate [CoW₁₁O₃₉(CpTi)] 7-(Cp= η^5 -C₅H₅). *J Inorg Biochem* 94(3):279–284
- Boulmier A et al (2017) Anticancer activity of polyoxometalate-bisphosphonate complexes: synthesis, characterization, in vitro and in vivo results. *Inorg Chem* 56(13):7558–7565
- Yamase TJME (1993) Polyoxometalates for molecular devices: antitumor activity and luminescence. *Mol Eng* 3(1–3):241–262
- Yamase T (2013) Polyoxometalates active against tumors, viruses, and bacteria. *Prog Mol Subcell Biol* 54:65–116
- Kalita A, Roch-Marchal C, Murugavel R (2013) Cationic D4R zinc phosphate-anionic polyoxometalate hybrids: synthesis, spectra, structure and catalytic studies. *Dalton Trans* 42(26):9755–9763
- Gerth HUV et al (2005) Cytotoxic effects of novel polyoxotungstates and a platinum compound on human cancer cell lines. *Anticancer Drugs* 16(1):101–106
- Sun X et al (2010) CD39/ENTPD1 expression by CD4+Foxp3+ regulatory T cells promotes hepatic metastatic tumor growth in mice. *Gastroenterology* 139(3):1030–1040
- Liu JC et al (2021) Multicomponent self-assembly of a giant heterometallic polyoxotungstate supercluster with antitumor activity. *Angew Chem Int Ed Engl* 60(20):11153–11157
- Van Rompuy LS, Parac-Vogt TN (2019) Interactions between polyoxometalates and biological systems: from drug design to artificial enzymes. *Curr Opin Biotechnol* 58:92–99
- She S et al (2016) Degradable organically-derivatized polyoxometalate with enhanced activity against glioblastoma cell line. *Sci Rep* 6:33529
- Zhang ZM et al (2016) Cation-mediated optical resolution and anticancer activity of chiral polyoxometalates built from entirely achiral building blocks. *Chem Sci* 7(7):4220–4229
- Prudent R et al (2008) Identification of polyoxometalates as nanomolar noncompetitive inhibitors of protein kinase CK2. *Chem Biol* 15(7):683–692
- Stephan H et al (2013) Polyoxometalates as versatile enzyme inhibitors. *Eur J Inorg Chem* 2013(10–11):1585–1594
- Joshi A et al (2020) Effective inhibitory activity against MCF-7, A549 and HepG2 cancer cells by a phosphomolybdate based hybrid solid. *Dalton Trans* 49(21):7069–7077
- Xue YR et al (2021) A hybrid HPV capsid protein L1 with giant Mo-containing polyoxometalate improves the stability of virus-like particles and the anti-tumor effect of [Mo(154)]. *Biomater Sci* 9(10):3875–3883
- Heidelberger C et al (1957) Fluorinated pyrimidines, a new class of tumour-inhibitory compounds. *Nature* 179(4561):663
- Fan X et al (2012) Synthesis, characterization and antitumor activity of rare earth Eu³⁺ and Dy³⁺ complexes with quercetin. In: *Proceedings of the 2012 international conference on biomedical engineering and biotechnology*. IEEE Computer Society. pp 567–569
- Breibeck J et al (2019) Keggin-type polyoxotungstates as mushroom tyrosinase inhibitors—a speciation study. *Sci Rep* 9(1):5183
- Li J et al (2005) A novel 5-fluorouracil salt of 12-silicatungstic acid: synthesis, structure characterization and antitumor activity. *Chem Res Chin Univ* 21(2):127
- Pałasz A, Czekaj P (2000) Toxicological and cytophysiological aspects of lanthanides action. *Acta Biochim Pol* 47(4):1107–1114
- Xia RY et al (2017) K(9)(C(4)H(4)FN(2)O(2))(2)Nd(PW(11)O(39))(2)·25H(2)O induces apoptosis in human lung cancer A549 cells. *Oncol Lett* 13(3):1348–1352

40. Yang HK et al (2013) Polyoxometalate–biomolecule conjugates: a new approach to create hybrid drugs for cancer therapeutics. *Bioorg Med Chem Lett* 23(5):1462–1466
41. Li C et al (2016) BSA-binding properties and anti-proliferative effects of amino acids functionalized polyoxomolybdates. *Biomed Pharmacother* 79:78–86
42. Kortz U et al (2002) Heteropolymolybdates of AsIII, SbIII, BiIII, SeIV, and TeIV functionalized by amino acids. *Angew Chem Int Ed* 41(21):4070–4073
43. Wang L et al (2019) The synthesis and biological function of a novel sandwich-type complex based on SbW(9) and flexible bpp ligand. *Adv Healthc Mater* 8(18):e1900471
44. Duncan R (2006) Polymer conjugates as anticancer nanomedicines. *Nat Rev Cancer* 6(9):688
45. Jayakumar R et al (2010) Novel carboxymethyl derivatives of chitin and chitosan materials and their biomedical applications. *Prog Mater Sci* 55(7):675–709
46. Kean T, Thanou MJ (2010) Biodegradation, biodistribution and toxicity of chitosan. *Adv Drug Deliv Rev* 62(1):3–11
47. Menon D et al (2011) A novel chitosan/polyoxometalate nano-complex for anti-cancer applications. *Carbohydr Polym* 84(3):887–893
48. Geisberger G et al (2013) Trimethyl and carboxymethyl chitosan carriers for bio-active polymer–inorganic nanocomposites. *PLoS ONE* 9(1):58–67
49. Song YF, Tsunashima RJ (2012) Recent advances on polyoxometalate-based molecular and composite materials. *Chem Soc Rev* 41(22):7384
50. Pérez-Álvarez L et al (2019) Chitosan nanogels as nanocarriers of polyoxometalates for breast cancer therapies. *Carbohydr Polym* 213:159–167
51. Pandya V, Joshi S (2017) Fabrication of novel anticancer polyoxometalate [CoW10O39(CpTi)]7-chitosan nanocomposite, its toxicity reduction, and sustained release. *Asian J Pharm Clin Res* 10(4):278
52. Zamolo VA et al (2018) Selective targeting of proteins by hybrid polyoxometalates: interaction between a bis-biotinylated hybrid conjugate and avidin. *Front Chem* 6:278
53. Levy M, Benita SJ (1989) Design and characterization of a sub-micronized o/w emulsion of diazepam for parenteral use. *Int J Pharm* 54(2):103–112
54. Zhai F et al (2008) Synthesis and characterization of polyoxometalates loaded starch nanocomplex and its antitumoral activity. *Eur J Med Chem* 43(9):1911–1917
55. Wang X et al (2005) New liposome-encapsulated-polyoxometalates: synthesis and antitumoral activity. *J Inorg Biochem* 99(2):452–457
56. Razavi SF et al (2020) Nanolipid-loaded Preyssler polyoxometalate: synthesis, characterization and invitro inhibitory effects on HepG2 tumor cells. *Toxicol In Vitro* 68:104917
57. Gabas IM et al (2016) In vitro cell cytotoxicity profile and morphological response to polyoxometalate-stabilized gold nanoparticles. *New J Chem* 40(2):1039–1047
58. Tang W et al (2018) Acidity/reducibility dual-responsive hollow mesoporous organosilica nanoplatfoms for tumor-specific self-assembly and synergistic therapy. *ACS Nano* 12(12):12269–12283
59. Zhou J et al (2020) Folin-ciocalteu assay inspired polyoxometalate nanoclusters as a renal clearable agent for non-inflammatory photothermal cancer therapy. *ACS Nano* 14(2):2126–2136
60. Isakovic AM et al (2021) Selected polyoxopalladates as promising and selective antitumor drug candidates. *J Biol Inorg Chem* 26(8):957–971
61. Zheng Y et al (2019) Self-assembly and antitumor activity of a polyoxovanadate-based coordination nanocage. *Chemistry* 25(67):15326–15332
62. Tagliavini V et al (2021) Enhancing the biological activity of polyoxometalate–peptide nano-fibrils by spacer design. *RSC Adv* 11(9):4952–5495
63. World AIDS Day—December 1, 2019. *MMWR Morb Mortal Wkly Rep* 68(47):1089
64. Wang X et al (2018) Inhibition of human immunodeficiency virus type 1 entry by a Keggin polyoxometalate. *Viruses* 10(5):265/1–265/15
65. Hill CL, Weeks MS, Schinazi RF (1990) Anti-HIV-1 activity, toxicity, and stability studies of representative structural families of polyoxometalates. *J Med Chem* 33(10):2767–2772
66. Judd DA et al (2001) Polyoxometalate HIV-1 protease inhibitors. A new mode of protease inhibition. *J Am Chem Soc* 123(5):886–897
67. Fukuma M, Seto Y, Yamase T (1991) In vitro antiviral activity of polyoxotungstate (PM-19) and other polyoxometalates against herpes simplex virus. *Antivir Res* 16(4):327–339
68. Ikeda S et al (1993) Activity of the keggin polyoxotungstate PM-19 against herpes simplex virus type 2 infection in immunosuppressed mice: role of peritoneal macrophage activation. *J Med Virol* 41(3):191–195
69. Dan K et al (2002) The memory effect of heteropolyoxotungstate (PM-19) pretreatment on infection by herpes simplex virus at the penetration stage. *Pharmacol Res* 46(4):357–362
70. Dan K, Yamase T (2006) Prevention of the interaction between HVEM, herpes virus entry mediator, and gD, HSV envelope protein, by a Keggin polyoxotungstate, PM-19. *Biomed Pharmacother* 60(4):169–173
71. Wang J et al (2014) Broad-spectrum antiviral property of polyoxometalate localized on a cell surface. *ACS Appl Mater Interfaces* 6(12):9785–9789
72. Li Q et al (2019) Antiviral effects of a niobium-substituted heteropolytungstate on hepatitis B virus-transgenic mice. *Drug Dev Res* 80(8):1062–1070
73. Wang J et al (2014) Pharmacokinetics of anti-HBV polyoxometalate in rats. *PLoS ONE* 9(6):e98292/1–e98292/9
74. Qi Y et al (2013) Inhibition of hepatitis C virus infection by polyoxometalates. *Antivir Res* 100(2):392–398
75. Qi Y et al (2020) Anti-flavivirus activity of polyoxometalate. *Antivir Res* 179:104813
76. Shigeta S et al (1996) In-vitro antimyxovirus activity and mechanism of anti-influenza virus activity of the polyoxometalates PM-504 and PM-523. *Antivir Chem Chemother* 7(6):346–352
77. Shigeta S et al (1997) Synergistic anti-influenza virus A (H1N1) activities of PM-523 (polyoxometalate) and ribavirin in vitro and in vivo. *Antimicrob Agents Chemother* 41(7):1423–1427
78. Shigeta S et al (2006) Anti-RNA virus activity of polyoxometalates. *Biomed Pharmacother* 60(5):211–219
79. Hosseini SM et al (2012) Anti-influenza activity of a novel polyoxometalate derivative (POM-4960). *Int J Mol Cell Med* 1(1):21–29
80. Liu J et al (2004) Synthesis, characterization and antiviral activity against influenza virus of a series of novel manganese-substituted rare earth borotungstates heteropolyoxometalates. *Antivir Res* 62(1):65–71
81. Inoue M et al (2006) Enhancement of antibacterial activity of beta-lactam antibiotics by [P2W18O62]6-, [SiMo12O40]4-, and [Pt12W10O40]7—against methicillin-resistant and vancomycin-resistant *Staphylococcus aureus*. *J Inorg Biochem* 100(7):1225–1233
82. Inoue M et al (2006) Synergistic effect of polyoxometalates in combination with oxacillin against methicillin-resistant and vancomycin-resistant *Staphylococcus aureus*: a high initial inoculum of 1 x 10⁸ cfu/ml for in vivo test. *Biomed Pharmacother* 60(5):220–226

83. Tajima Y (2001) Lacunary-substituted undecatungstosilicates sensitize methicillin-resistant *Staphylococcus aureus* to beta-lactams. *Biol Pharm Bull* 24(9):1079–1084
84. Inoue M et al (2005) Antibacterial activity of highly negative charged polyoxotungstates, K₂₇[KAs₄W₄₀O₁₄₀] and K₁₈[KSb₉W₂₁O₈₆], and Keggin-structural polyoxotungstates against *Helicobacter pylori*. *J Inorg Biochem* 99(5):1023–1031
85. Barsukova-Stuckart M et al (2012) Synthesis and biological activity of organoantimony(III)-containing heteropolytungstates. *Inorg Chem* 51(21):12015–12022
86. Yang P et al (2016) 19-Tungstodiarsenate(III) functionalized by organoantimony(III) groups: tuning the structure-bioactivity relationship. *Inorg Chem* 55(1):251–258
87. Shahid M et al (2014) Isolation of a decavanadate cluster [H₂V₁₀O₂₈][4-picH]·4·2H₂O (4-pic = 4-picoline): crystal structure, electrochemical characterization, genotoxic and antimicrobial studies. *J Cluster Sci* 25(5):1435–1447
88. Fiorani G et al (2014) Chitosan-polyoxometalate nanocomposites: synthesis, characterization and application as antimicrobial agents. *J Cluster Sci* 25(3):839–854
89. Zhang C et al (2020) An enhanced antibacterial nanoflowers AgPW@PDA@Nisin constructed from polyoxometalate and nisin. *J Inorg Biochem* 212:111212
90. Xu Z et al (2020) Sustained release of Ag(+) confined inside polyoxometalates for long-lasting bacterial resistance. *Chem Commun (Camb)* 56(39):5287–5290
91. Daima HK et al (2013) Fine-tuning the antimicrobial profile of biocompatible gold nanoparticles by sequential surface functionalization using polyoxometalates and lysine. *PLoS ONE* 8(10):e79676
92. Daima HK et al (2014) Synergistic influence of polyoxometalate surface corona towards enhancing the antibacterial performance of tyrosine-capped Ag nanoparticles. *Nanoscale* 6(2):758–765
93. Bijelic A, Aureliano M, Rompel A (2018) The antibacterial activity of polyoxometalates: structures, antibiotic effects and future perspectives. *Chem Commun (Camb)* 54(10):1153–1169
94. Gao N et al (2014) Transition-metal-substituted polyoxometalate derivatives as functional anti-amyloid agents for Alzheimer's disease. *Nat Commun* 5:4422/1-4422/9
95. Li M et al (2013) Self-assembled peptide-polyoxometalate hybrid nanospheres: two in one enhances targeted inhibition of amyloid β -peptide aggregation associated with Alzheimer's disease. *Small* 9(20):3455–3461
96. Li M et al (2017) Using multifunctional peptide conjugated Au nanorods for monitoring β -amyloid aggregation and chemophotothermal treatment of Alzheimer's disease. *Theranostics* 7(12):2996–3006
97. Guan Y et al (2016) Ceria/POMs hybrid nanoparticles as a mimicking metalloproteinase for treatment of neurotoxicity of amyloid- β peptide. *Biomaterials* 98:92–102
98. Chen Q et al (2014) Mo polyoxometalate nanoclusters capable of inhibiting the aggregation of A β -peptide associated with Alzheimer's disease. *Nanoscale* 6(12):6886–6897
99. Zhao J et al (2019) Organoplatinum-substituted polyoxometalate inhibits β -amyloid aggregation for Alzheimer's therapy. *Angew Chem Int Ed Engl* 58(50):18032–18039
100. Liu Y et al (2019) Peptide-modified Mo polyoxometalate nanoparticles suppress Zn²⁺-induced A β aggregation. *ChemNanoMat* 5(7):897–910
101. Ma M et al (2018) Redox-activated near-infrared-responsive polyoxometalates used for photothermal treatment of Alzheimer's disease. *Adv Healthc Mater* 7(20):e1800320
102. Čolović MB et al (2017) Toxicity evaluation of two polyoxotungstates with anti-acetylcholinesterase activity. *Toxicol Appl Pharmacol* 333:68–75
103. Iqbal J et al (2013) Polyoxometalates as potent inhibitors for acetyl and butyrylcholinesterases and as potential drugs for the treatment of Alzheimer's disease. *Med Chem Res* 22(3):1224–1228
104. Bondžić AM et al (2020) A new acetylcholinesterase allosteric site responsible for binding voluminous negatively charged molecules - the role in the mechanism of AChE inhibition. *Eur J Pharm Sci* 151:105376

Publisher's Note Springer Nature remains neutral with regard to jurisdictional claims in published maps and institutional affiliations.

Authors and Affiliations

Xuechen Wang¹ · Shengnan Wei¹ · Chao Zhao¹ · Xin Li¹ · Jin Jin¹ · Xuening Shi¹ · Zhenyue Su¹ · Juan Li¹ · Juan Wang¹

✉ Juan Li
li_juan@jlu.edu.cn

✉ Juan Wang
jwang0723@jlu.edu.cn

¹ School of Public Health, Jilin University, Changchun, Jilin, China